Biochemical Pharmacology 83 (2012) 324–334

Contents lists available at SciVerse ScienceDirect

Biochemical Pharmacology

journal homepage: www.elsevier.com/locate/biochempharm

Differential expression and roles of volume-activated chloride channels in control of growth of normal and cancerous nasopharyngeal epithelial cells

Linyan Zhu [a,1], Haifeng Yang [b,1], Wanhong Zuo [a], Linjie Yang [a], Haifeng Zhang [a], Wencai Ye [c], Jianwen Mao [d], Lixin Chen [a,*], Liwei Wang [a,*]

[a] Medical College, Jinan University, Guangzhou 510632, China
[b] Department of Pathology, The Second Affiliated Hospital of Guangzhou University of Chinese Medicine (Guangdong Provincial Hospital of TCM), Guangzhou 510120, China
[c] College of Pharmacy, Jinan University, Guangzhou 510632, China
[d] Department of Biology, Guangdong Pharmaceutical University, Guangzhou, China

ARTICLE INFO

Article history:
Received 8 September 2011
Accepted 8 November 2011
Available online 18 November 2011

Keywords:
Cancer
Chloride channels
Cell proliferation
ClC-3
Nasopharyngeal carcinoma

ABSTRACT

We have previously shown that chloride channel activities were cell cycle-dependent and were involved in cell proliferation in nasopharyngeal carcinoma cells. In this study, the expression and roles of volume-activated chloride channels in cell growth were investigated in the poorly-differentiated human nasopharyngeal carcinoma cell (CNE-2Z) and its counterpart, the normal human nasopharyngeal epithelial cell (NP69-SV40T). Consistent with growth ability, the background chloride currents recorded under isotonic condition, the volume-activated chloride currents induced by 47% hypotonic challenges and the hyponinicity-induced regulatory volume decrease (RVD) were much larger in CNE-2Z cells than in NP69-SV40T cells, suggesting the up-regulation of expression of volume-activated chloride channels in cancerous cells. This was proved by the up-regulation of ClC-3 proteins, a candidate of volume-activated chloride channels, in the cancerous cells. Functional inhibition of chloride channel activities by the chloride channel blockers, 5-nitro-2-(3-phenylpropylamino)benzoic acid (NPPB) and tamoxifen, and knock-down of ClC-3 expression by specific ClC-3 siRNA attenuated the background currents, suppressed the activation of volume-activated chloride currents, decreased the hyponinicity-induced RVD and inhibited cell growth in the cancerous and normal cells. However, the sensitivities of the cancerous cells were much higher than that of the normal cells. Our data suggest that volume-activated chloride channels play a more important role in control cell proliferation in the cancerous cells than in the normal cells; the growth of cancerous cells is more dependent on the activities of volume-activated chloride channels than that of the normal cells. ClC-3 protein may be considered as a potential tumor marker and therapeutic target for human nasopharyngeal carcinoma

1. Introduction

Ion channels are membrane proteins controlling massive ion fluxes across plasma membranes and participating in diverse physiological events such as excitability, contraction, cell cycle and metabolism both in health and disease [1]. Recently, studies suggest that most human neoplastic cells show altered expression of a variety of ion channels and that these channels exert different functional roles [2,3]. The physiological expression of the ether à go-go (EAG) channel is restricted to the brain but it is frequently and abundantly expressed in many solid tumors, thereby making it a promising target for a specific diagnosis and therapy [4]. In myeloblastic leukemia cells, voltage-gated K^+ currents vanished during cell differentiation [5]. The expression of the adenosine triphosphate (ATP)-sensitive potassium channel in glioma tissues was greatly increased and down-regulation of this channel by small interfering RNA (siRNA) inhibited glioma cell proliferation [6].

Chloride channels express ubiquitously and have been suggested to play a role in cell proliferation [7–13]. In our previous work, we demonstrated that the expression of volume-activated chloride current ($I_{Cl.vol}$) was cell cycle-dependent and cell proliferation was positively correlated with the level of $I_{Cl.vol}$ in poorly-differentiated nasopharyngeal carcinoma cells [14,15].

Although the molecular nature that provide the $I_{Cl.vol}$ is still unidentified, evidences, including our own strongly support that ClC-3, a member of the ClC family of voltage-gated Cl^- channels, is one such molecular candidate [16–18]. ClC-3 protein expression

* Corresponding author. Tel.: +86 20 85220260; fax: +86 20 85221343.
E-mail addresses: chenlixinw@sohu.com (L. Chen), wangliweic@sohu.com (L. Wang).
[1] These authors contributed equally to this work.

0006-2952/$ – see front matter © 2011 Elsevier Inc. All rights reserved.
doi:10.1016/j.bcp.2011.11.007

has been found in different cancer cell types, including prostate cancer epithelial cells [19], PC12 cells [20], glioma cells [21] and CNE-2Z cells [22]. Our previous work and the data of other laboratories indicated that expression of ClC-3 was cell cycle dependent [22]. ClC-3 was a critical regulator of the cell cycle [23]. ClC-3 may play its roles in regulation of cell proliferation by altering $I_{Cl.vol}$ and RVD [24]. ClC-3 null mice exhibited a complex phenotype, including poor growth, hippocampal degeneration, seizures, kyphosis, and retinal blindness [25–27].

Much attention has been paid to the expression and involvement of chloride channels in proliferation in cancer cells. The immediately arising question was whether chloride channel expression in tumor cells was a consequence of the abnormal growth, or whether the channels were necessary for cell proliferation and play more important role in cancer cells than in normal cells. This study was performed to evaluate and compare the expression and functional activities of volume-activated channels between normal and cancerous nasopharyngeal epithelial cells. We chose two cell lines, NP69-SV40T and CNE-2Z, derived from normal and carcinoma nasopharyngeal epithelium, which represent different proliferative capacity and carcinogenic potential. The CNE-2Z cell line possesses high potential to generate tumors in host tissues, but the NP69-SV40T cell line is non-tumorigenic. The NP69-SV40T cell line maintains characteristics of primary nasopharyngeal epithelial cells such as anchorage-dependent growth and is frequently used as the normal cell model of nasopharyngeal epithelial cells [28,29]. In this study, functional inhibition of chloride channels by channel blockers and suppression of ClC-3 expression by small interfering RNA are used to estimate the role of ClC-3 in cell proliferation in the normal and cancerous cells.

2. Materials and methods

2.1. Cell culture

The poorly differentiated human nasopharyngeal carcinoma cell line, CNE-2Z, was kindly provided by Professor Weiping Tang (Department of Pathology, Guangdong Medical College, China). The immortalized human nasopharyngeal epithelial cell line (NP69-SV40T), which was derived from the normal nasopharyngeal epithelium and established by Tsao et al. [28], was obtained from Hunan Xiangya Type Culture Collection (Hunan, China). Both cells were grown in the RPMI 1640 medium supplemented with 10% new-born calf serum (Gibco, Grand Island, USA), 100 units/ml penicillin G and 100 μg/ml streptomycin (Sigma–Aldrich, St. Louis, MO, USA) at 37 °C in a humidified atmosphere containing 5% CO_2. Cells were seeded in 25-cm^2 flasks and sub-cultured every other day.

2.2. Detection of ClC-3 by Western blotting

Cells were washed with ice-cold PBS and lysed with buffer containing Tris–Cl (50 mM), NaCl (150 mM), NaN_3 (0.02%), Nonidet P-40 (1%), sodium deoxycholate (1%), SDS (0.1%), leupeptin (5 μg/ml) and aprotinin (1 μg/ml). Equal amounts of proteins were separated by 8% SDS-PAGE, transferred to polyvinylidene-fluoride (PVDF) membranes (Millipore, Bedford, MA, USA) and incubated with rabbit anti-ClC-3 primary antibody (1:300, Alomone Labs, Jerusalem, Israel) and mouse anti-actin antibody (1:1000, Boster Bio-technology Co., Ltd., Wuhan, China) overnight at 4 °C. Proteins were visualized with the HRP-linked goat anti-rabbit secondary antibody (1:1000, Proteintech Group, Inc., Chicago, USA) and the HRP-linked goat anti-mouse IgG (1:1000, Proteintech Group, Inc., Chicago, USA). Final detection was accomplished with Western blot luminol reagent (Millipore, Bedford, MA, USA). The density of target bands was quantified by the computer-aided 1D gel analysis system. ClC-3 immunoreactivity was normalized to β-actin.

2.3. Immunofluorescence

For immunofluorescence, cells were plated on 6 mm round glass coverslips and cultured in 24-well plates for 24 h before fixation with paraformaldehyde (4%) and sucrose (0.12 M) in PBS. Cells were permeabilized with Triton X-100 (0.3% in PBS) and blocked with 10% normal sheep serum (Sigma–Aldrich, St. Louis, MO, USA) in PBS for 45 min. Cells were then covered with the rabbit anti-ClC-3 primary antibody (1:50, Alomone Labs, Jerusalem, Israel) overnight at 4 °C. Afterwards, the cells were incubated in FITC conjugated goat anti-rabbit secondary antibody (1:50, Proteintech Group, Inc., Chicago, USA) and DAPI (5 μg/ml, Beyotime Institute of Biotechnology, Haimen, China) at room temperature. Finally, the coverslips with cells were inverted onto glass slides, sealed with nail varnish and examined by a confocal microscope (C1 Si, Nikon, Tokyo, Japan). The focus was adjusted until the peak signal was obtained, then the images were acquired. To obtain a good signal-to-noise ratio, 4 frames were averaged before image acquisition. The fluorescence intensity (grey level) of the fluorescence images of each individual cell was measured by using NIS-Elements AR image analysis system (Nikon, Tokyo, Japan).

2.4. Down-regulation of ClC-3 expression by siRNA interference

Compared with that of the antisense technique, the efficiency of the small RNA interference (siRNA) technique is higher. The working concentrations of siRNA and transfect reagents used in siRNA experiments are much lower than those of oligonucleotides and transfect reagents needed for antisense experiments, resulting in a lower side effect for the siRNA approach. The application of the antisense technique has been gradually replaced by the siRNA approach in recent years. In this study, the small RNA interference (siRNA) technique was used to knock down ClC-3 expression. The sequences of siRNA duplexes of 21-nucleotide were: sense, (5′–3′) CAAUGGAUUUCCUGUCAUATT; antisense, (5′–3′) UAUGACAG-GAAAUCCAUUGTA. The negative control siRNA, that does not recognize any known target to mammalian genes, was: sense, (5′–3′) UUC UCC GAA CGU GUC ACG UTT; antisense, (5′–3′) ACG UGA CAC GUU CGG AGA ATT. siRNAs were synthesized and labeled with FAM carboxyfluorescein by GenePharma (GenePharma.Co., Ltd, Shanghai, China). The transfection reagent Lipofectamine 2000 (Invitrogen, Carlsbad, CA, USA) was used to facilitate siRNA transfection. Cells were transfected with indicated concentrations of ClC-3 siRNA or negative control siRNA plus lipofectamine 2000 (1 μl in 500 μl medium for 24-well plate and 0.25 μl in 100 μl medium for 96-well plate) in serum and antibiotics-free culture medium for 6 h and incubated in normal RPMI 1640 medium containing serum at 37 °C in a CO_2 incubator for 48 h before the experiments of electrophysiology, immunofluorescence, cell volume analysis and MTT assay.

2.5. Electrophysiological recordings

For the experiments, the cell suspension was plated onto round coverslips with a diameter of 22 mm, and incubated at 37 °C for about 1–2 h before being used for current recordings. The whole-cell mode of the patch clamp technique was used to measure membrane currents with an EPC-7 amplifier (HEKA, Darmstadt, Germany). Patch pipettes were manufactured from standard wall borosilicate glass capillaries with an inner filament (Clark Electromedical Instruments, Kent, UK) on a two-stage vertical puller (PB-7, Narishige, Tokyo, Japan) and gave a

resistance of 4–5 MΩ when filled with the pipette solution. The liquid junction potential was corrected when the pipette entered the bath and the access resistance was compensated. The whole cell capacitance was determined by adjusting and minimizing the capability transients in response to a 20 mV voltage step. Once the whole-cell configuration was established, the current–voltage relationship and time course of the current were obtained from a series of voltage steps applied repeatedly. Cells were held at the Cl^- equilibrium potential (E_{Cl}; 0 mV) and then stepped repeatedly to 0, ±40 and ±80 mV, with a 200 ms duration for each step and 4 s intervals between steps. To analyze the *I–V* relationship in more detail, 1 s voltage steps from −120 mV to +120 mV with an increment of 20 mV were applied. The command voltages and whole cell currents were recorded simultaneously on a computer via a laboratory interface (CED 1401, Cambridge, UK) with a sampling rate of 3 kHz. The voltage pulse generation, data collection, and current analysis were performed by the EPC software package (CED, Cambridge, UK). In analysis of the data collected, all current measurements were made at 10 ms after the onset of each voltage step. Current densities were determined by normalizing the whole-cell current to the membrane capacitance.

2.6. Cell proliferation assays

3-(4,5-Dimethyl-thiazol-2-yl)-2,5-diphenyl tetrazolium bromide (MTT, Sigma–Aldrich, St. Louis, MO, USA) assay was applied to assess the effects of chloride channel blocker and ClC-3 siRNA on cell proliferation. Cells were seeded into 96-well plates at a density of 5000 cells per well with culture volume of 100 μl and cultured for 14 h. The cells were treated with the media containing different reagents for 24–72 h. 10 μl stock solution of MTT (5 mg/ml) was added to each well and incubated at 37 °C for 4 h. Medium was removed, and 100 μl of DMSO was added into each well to dissolve the purple formazan crystals. The absorbance (expressed as optical density, OD) was recorded and quantified at 570 nm by an automated plate reader (Model 680, BIO-RAD, CA, USA). Results were standardized using control group values.

2.7. Measurements of cell volume

The coverslip with cells was stuck to the base of a perfusion chamber and mounted onto an inverted phase-contrast microscope (Leitz DMIL; Leica Mikroskopie und Systeme GmbH, Wetzlar, Germany). The bath volume was 0.2 ml and solution was supplied by continuous perfusion with an inflow rate of 2 ml/min. All experiments were carried out at room temperature (24–26 °C). Cell images were captured every 30 s by a CCD digital camera (Mono CCD625, Leica, Wetzlar, Germany) that was connected to the microscope and stored directly onto the computer. The acquisition of cell images was controlled by the Quantimet Q500MC image processor, and the images of each individual cell (except the cells with unclear edges) were later analyzed by the imaging software (Leica, Wetzlar, Germany). The cell volume was calculated from cell diameters (d) with the equation $V = 4/3\pi \times (d/2)^3$. RVD was calculated as follows: $\text{RVD}\ (\%) = (V_{max} - V_{min})/(V_{max} - V_0) \times 100\%$, where V_0 is the cell volume in isotonic solution before hypotonic shocks, V_{max} the peak volume in hypotonic solutions, V_{min} the volume before returning to isotonic solution. Cell volume was standardized to the time point before exposed to the hypotonic solution.

2.8. Solutions

The pipette solution contained (in mM): 70 N-methyl-D-glucamine chloride (NMDG-Cl), 1.2 $MgCl_2$, 10 HEPES, 1 EGTA, 140 D-mannitol and 2 ATP. The isotonic bath solution contained (in mM): 70 NaCl, 0.5 $MgCl_2$, 2 $CaCl_2$, 10 HEPES and 140 D-mannitol. The osmolarity of pipette and isotonic bath solutions was adjusted to 300 mOsmol/L with D-mannitol, and the osmolarity of solutions was measured with a freezing-point osmometer (OSMOMAT 030; Gonotec GmbH, Berlin, Germany). 47% hypotonic solution was obtained by omitting 140 D-mannitol from the isotonic bath solution with the osmolarity of 160 mOsmol/L. The pH of the pipette and bath solutions was adjusted to 7.25 and 7.4, respectively, with 1 M Tris-base. The chloride channel blockers, 5-nitro-2-(3-phenylpropylamino) benzoic acid (NPPB) and tamoxifen were dissolved in dimethyl sulfoxide (DMSO) and methanol at the concentration of 100 mM and 50 mM, respectively, and diluted to the indicated final concentrations with bath solutions. All chemicals were obtained from Sigma (Sigma–Aldrich, St. Louis, MO, USA).

2.9. Statistics

Data were expressed as mean ± standard error (number of observations) and were analyzed using the analysis of variance (ANOVA). $P < 0.05$ was considered significant. All experiments were repeated at least 3 times.

3. Results

3.1. Differential growth ability and contribution of chloride channels in control of cell growth in normal and cancerous nasopharyngeal epithelial cells

Fig. 1A shows that both cells grew well in the medium, but the normal nasopharyngeal epithelial cell, NP69-SV40T, proliferated much slower than the cancerous cells, CNE-2Z. Further experiments indicated that the growth of both cells was inhibited by the chloride channel blockers, NPPB (Fig. 1B–D) and tamoxifen (Fig. 1B, E and F). However, the cancerous cells were more sensitive to the blockers than the normal cells. 72 h after incubation in the culture medium with 100 μM NPPB, cell growth was inhibited by 13.3 ± 2.3% in NP69-SV40T cells ($P < 0.01$, $n = 3$) and by 51.9 ± 2.6% in CNE-2Z cells ($P < 0.01$, $n = 3$). The inhibitory effect of tamoxfen (20 μM) on cell growth was stronger than that of NPPB, with the inhibition rates of 45.5 ± 5.8% in NP69-SV40T cells ($P < 0.01$, $n = 3$) and 89.8 ± 6.1% in CNE-2Z cells ($P < 0.01$, $n = 3$). The results suggest that the activities of chloride channels or the roles of chloride channels in regulation of proliferation are different between the two cells.

3.2. Increased chloride currents in nasopharyngeal carcinoma cells

To evaluate the activities of the chloride channels in the normal and cancerous nasopharyngeal cells, whole-cell chloride currents were recorded in NP69-SV40T and CNE-2Z cells. The results showed that both cells exhibited background chloride currents in the isotonic condition and the currents could be activated further by extracellular applications of 47% hypotonic challenges (Fig. 2A and B). The hypotonicity-activated chloride currents were inhibited by the cell shrinkage induced by 47% hypertonic bath solution, indicating that the chloride currents were volume-sensitive.

However, further analysis indicated that current densities were different between the two cells. Both the background chloride current and the hypotonicity-activated chloride current in the normal cell (NP69-SV40T) were smaller than those in the cancerous cell (CNE-2Z) (Fig. 2B). The current densities of background and hypotonicity-activated chloride currents at +80 mV were 7.2 ± 1.7 and 41.8 ± 4.7 pA/pF in NP69-SV40T cells ($n = 9$) and were 14.1 ± 2.2 and 83.1 ± 10.6 pA/pF in CNE-2Z ($n = 9$). The results indicated that the functional expression of volume-activated chloride channels was up-regulated in the cancerous cells.

In both cells, the background and hypotonicity-activated chloride currents could be inhibited by the chloride channel

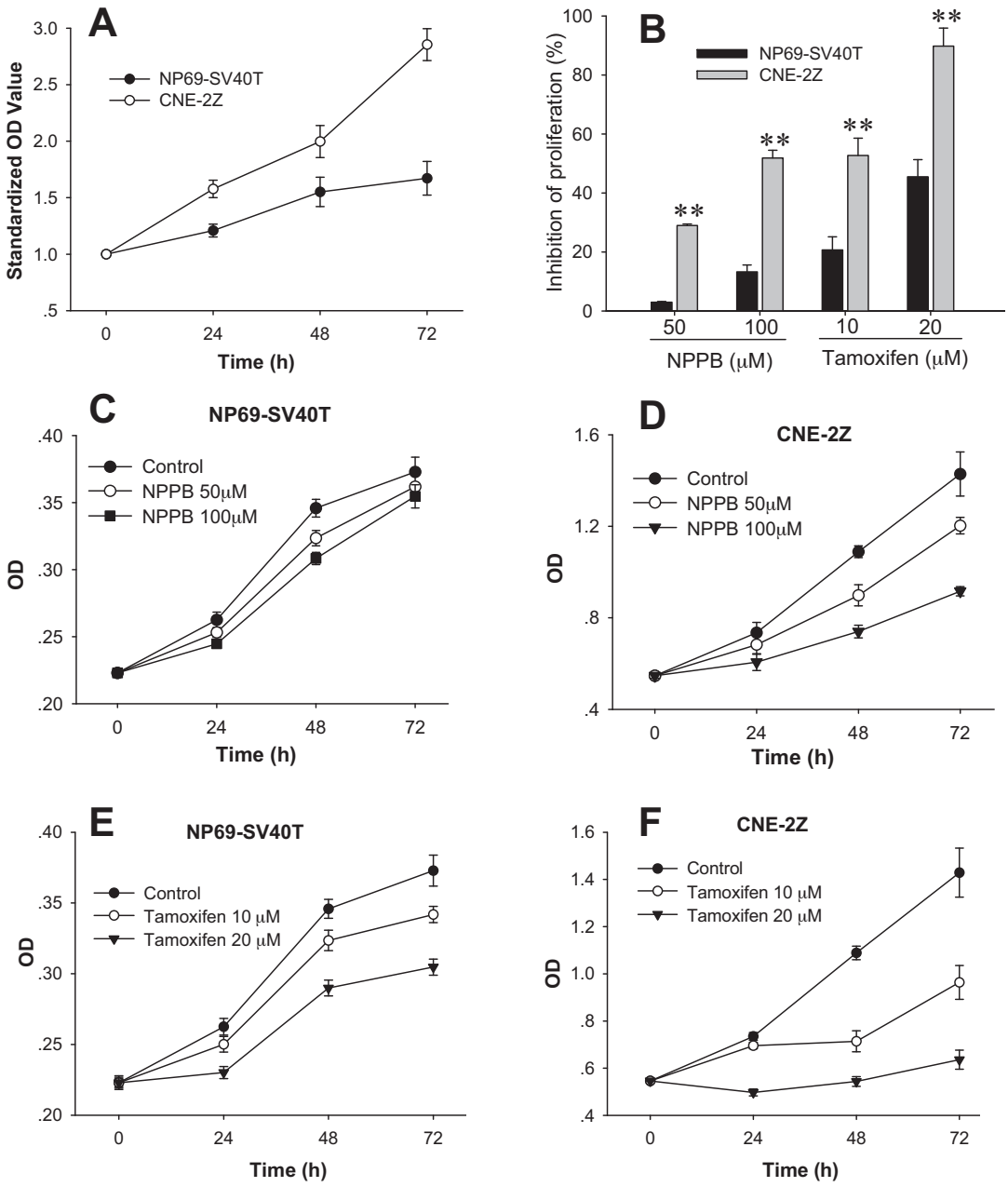

Fig. 1. Growth ability of NP69-SV40T and CNE-2Z cells in the normal culture medium and inhibition of cell proliferation by the chloride channel blockers NPPB and tamoxifen. Cells were cultured in 96-well culture plates (at a density of 3000 cells/well) in the normal medium overnight (about 16–18 h) and then incubated in the control medium or in the medium containing NPPB (50 and 100 μM) or tamoxifen (10 and 20 μM) for 72 h. The relative cell number was detected by the MTT assay and expressed with OD (optical density) values. (A) Shows the comparison of cell growth by standardized OD values at different time points between NP69-SV40T and CNE-2Z cells. (B–F) Present the inhibition of cell growth by NPPB and tamoxifen in the two cell lines. The data in the figures are the mean ± standard error of 3 experiments. $^{**}P < 0.01$ (*vs* NP69-SV40T).

blockers NPPB (100 μM) and tamoxifen (20 μM), as shown in Fig. 2C and F. Furthermore, the sensitivity of background and hypotonicity-activated currents to the chloride channel blockers was different between the two cells. The inhibition of the background and hypotonicity-activated currents at +80 mV in NP69-SV40T was slightly lower than those in CNE-2Z cells. In both cells, the inhibitory effect of tamoxifen (20 μM) was stronger than that of NPPB (100 μM).

3.3. Enhancement of regulatory volume decrease (RVD) in nasopharyngeal carcinoma cells

In our previous work, we demonstrated that volume-activated chloride channels play a pivotal role in the process of regulatory cell volume decrease (RVD) [30]. Here, we compared the RVD capability between the normal (NP69-SV40T) and cancerous (CNE-2Z) cells. The overall process of volume changes induced by 47% hypotonic solution in NP69-SV40T cells was similar to that in CNE-2Z cells. Following the 47% hypotonic stress, cell swelled immediately and then cell volume decreased gradually towards normal levels (Fig. 3). However, the extent of volume recovery was significantly different. The capability of RVD in CNE-2Z cells (58.3 ± 5.8%, 45 cells in 5 experiments) was significantly higher than that in NP69-SV40T cells (20.1 ± 6.7%, 89 cells in 6 experiments) ($P < 0.01$, Fig. 3A and B).

The chloride channel blockers NPPB and tamoxifen could inhibit the hypotonicity-induced RVD in both the normal and cancerous cells. As shown in Fig. 3C and D, the RVD induced

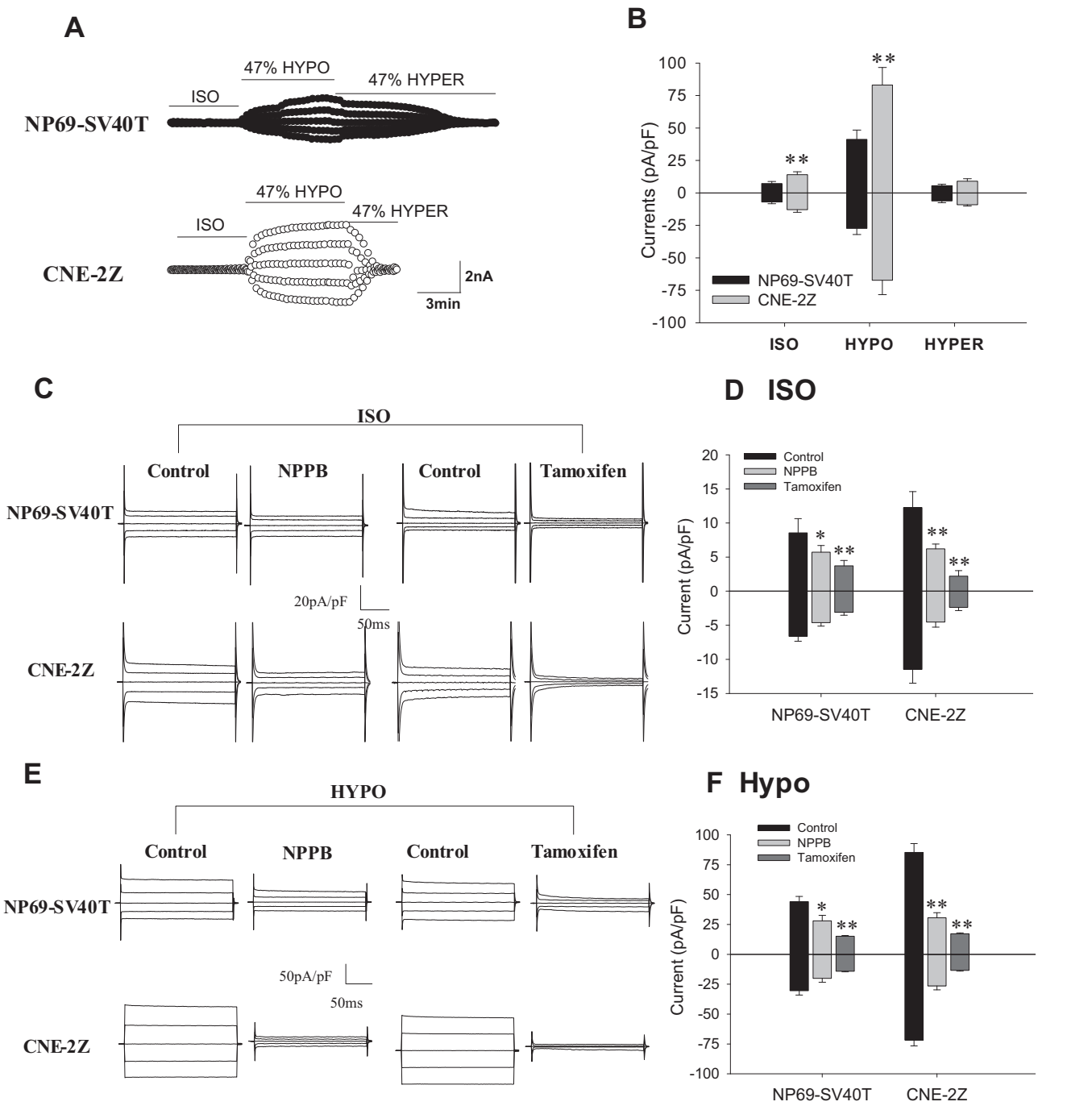

Fig. 2. Whole-cell chloride currents in CNE-2Z and NP69-SV40T cells. The voltage was held at 0 mV and then stepped repeatedly to 0, ±40 and ±80 mV with an interval of 4 s between steps. (A) Typical time-courses of chloride currents recorded in the isotonic (ISO), 47% hypotonic (47% HYPO) and 47% hypertonic (47% HYPER) bath solutions in NP69-SV40T and CNE-2Z cells. (B) Mean densities of the chloride currents recorded at ±80 mV under isotonic, hypotonic and hypertonic conditions. (C and D) Typical current traces (C) and mean densities at ±80 mV (D) of the background currents in the isotonic solution and the inhibitory effects of the chloride channel blockers NPPB (100 μM) and tamoxifen (20 μM) on the currents. (E and F) Typical current traces (E) and mean densities at ±80 mV (F) of the currents activated by 47% hypotonic challenges and the inhibitory effects of NPPB (100 μM) and tamoxifen (20 μM) on the currents. The data in B, D and F are mean ± standard error of 5–9 cells. $^{*}P < 0.05$; $^{**}P < 0.01$ (*vs* control).

by 47% hypotonic solution were inhibited significantly by 100 μM NPPB by 50.8 ± 8.4% (39 cells in 3 experiments, $P < 0.01$) in NP69-SV40T cells and 61.2 ± 7.8% (30 cells in 4 experiments, $P < 0.01$) in CNE-2Z cells. Further analysis indicated that additions of NPPB into the isotonic solution swelled both cells slightly (Fig. 3E). However, NPPB-induced cell swelling was stronger in CNE-2Z cells than in NP69-SV40T cells under normotonic conditions, suggesting that the activities of chloride channels in the normal isotonic condition were higher in cancerous cells than in normal cells. Tamoxifen (20 μM) could also affect the cell volume under the isotonic condition and inhibit the hypotonicity-induced RVD, but the effect was stronger than that of NPPB (Fig. 3F-H). The RVD was inhibited significantly by tamoxifen by 64.7 ± 9.7% (21 cells in 3 experiments, $P < 0.01$) in NP69-SV40T cells and 82.3 ± 8.4% (26 cells in 3 experiments, $P < 0.01$) in CNE-2Z cells.

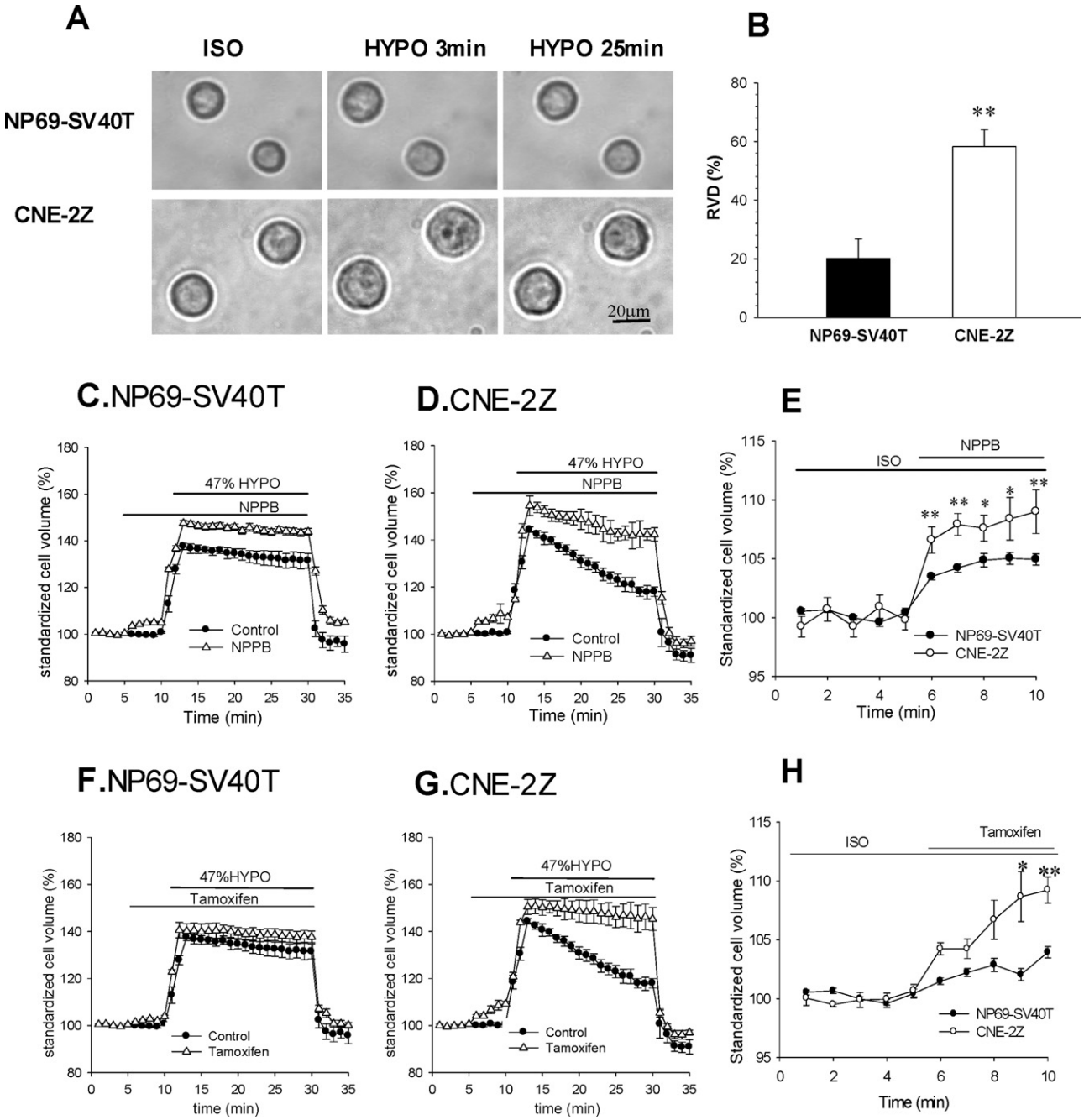

Fig. 3. Differential capability of regulatory volume decrease (RVD) and responses of cells to the chloride channel blockers NPPB and tamoxifen in NP69-SV40T and CNE-2Z cells. A presents the cell images taken in the isotonic solution (ISO) and in 47% hypotonic bath solution for 3 min (HYPO 3 min) and 25 min (HYPO 25 min) in NP69-SV40T (upper row) and CNE-2Z cells (lower row). (B) The RVD capacity in the hypotonic bath solution. (C, D and F, G) The changes of cell volume in the isotonic and hypotonic bath solutions without (control) or with 100 μM NPPB (NPPB) or 20 μM tamoxifen (tamoxifen) in NP69-SV40T and CNE-2Z cells, respectively. (E and H) The changes of cell volume induced by 100 μM NPPB (E) and 20 μM tamoxifen (H) under isotonic conditions. Note the higher sensitivity of CNE-2Z cells to NPPB and tamoxifen, compared with NP69-SV40T cells. The data in (B)–(H) are mean ± standard error of 21–89 cells. $^{*}P < 0.05$; $^{**}P < 0.01$ (*vs* NP69-SV40T).

3.4. Up-regulation of endogenous ClC-3 protein expression in nasopharyngeal carcinoma cells

The above results indicated that the functional activities of volume-sensitive chloride channels were up-regulated in nasopharyngeal carcinoma cells. To study further, the endogenous expression of ClC-3 protein, a candidate of the volume-activated chloride channel, was detected by Western blot and immunofluorescent analysis in NP69-SV40T and CNE-2Z cells using an antibody directed against ClC-3. The results of Western blot analysis showed that ClC-3 protein was expressed in both cell lines (Fig. 4A), but the expression level was significantly higher in CNE-2Z cells than in NP69-SV40T cells. Densitometric analysis indicated that the expression level of ClC-3 protein in CNE-2Z cells was 1.68 ± 0.44 folds of that in NP69-SV40T cells ($n = 3$, $P < 0.01$, Fig. 4B). The up-regulation of endogenous ClC-3 protein expression in CNE-2Z cells was further confirmed by immunofluorescent analysis using confocal microscopy (Fig. 5A). The ClC-3 immunofluorescence was detectable in both cell lines. However, the fluorescence in CNE-2Z cells was much stronger than that in NP69-SV40T cells. Analysis of

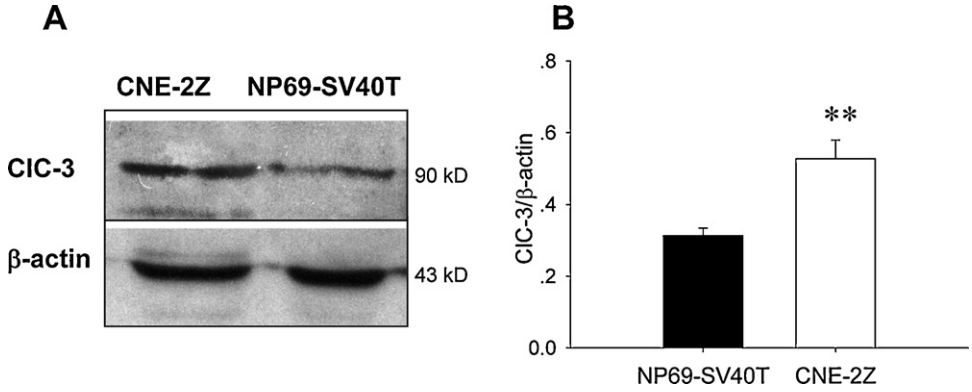

Fig. 4. ClC-3 protein expression in NP69-SV40T and CNE-2Z cells. The representative Western blotting for ClC-3 protein expression is presented in (A). Densitometry quantification of ClC-3 protein expression (intensity ratio of ClC-3 to β-actin) is shown in (B) (mean ± standard error, $n = 3$). $^{**}P < 0.01$ (*vs* NP69-SV40T).

immunofluorescent distribution indicated that ClC-3 proteins were located inside the cells, especially in the nuclei, as well as on the cell membrane.

3.5. Roles of ClC-3 proteins in activation of volume-activated chloride currents in normal and cancerous nasopharyngeal epithelial cells

To clarify the roles of ClC-3 proteins in activation of volume-activated chloride currents in normal and cancerous nasopharyngeal epithelial cells, the effects of knock down of ClC-3 expression on activation of volume-activated chloride currents were examined in NP69-SV40T and CNE-2Z cells. Specific ClC-3 siRNA was used to knock down the expression of ClC-3 proteins. Cells were treated with 100 nM ClC-3 siRNA or control siRNA in the presence of the transfection reagent lipofectamine 2000 for 48 h. The results showed that incubation of cells with specific ClC-3 siRNA successfully knocked down the expression of ClC-3 proteins in both cells (Fig. 5A). The nonsense control siRNA did not alter the expression of ClC-3 proteins.

To recognize the cells that were successfully transfected, ClC-3 siRNA and nonsense control siRNA were labeled with fluorescent FAM. FAM fluorescence in cells was detected with a florescent microscope. The results indicated that siRNA was successfully taken up by most of the CNE-2Z and NP69-SV40T cells (Fig. 5B).

48 h after treatments with 100 nM ClC-3 siRNA or nonsense control siRNA, the changes of whole cell chloride currents in the cells with fluorescence, indicating successful transfection of siRNA, were examined by the patch clamp technique (Fig. 6A). The treatments with nonsense control siRNA did not significantly affect the background chloride currents recorded under isotonic conditions and the volume-activated chloride currents induced by 47% hypotonic bath solution in the NP69-SV40T and CNE-2Z cells. However, the background and volume-activated chloride currents were significantly attenuated in the cells treated with specific ClC-3 siRNA.

With nonsense siRNA, the mean densities of background chloride currents in NP69-SV40T and CNE-2Z cells were 7.9 ± 1.9 ($n = 11$) and 10.9 ± 1.6 pA/pF ($n = 9$) at +80 mV. In the presence of specific ClC-3 siRNA, the currents decreased to 4.7 ± 0.9 pA/pF in NP69-SV40T cells ($n = 10$, $P < 0.01$) and 3.2 ± 0.7 pA/pF in CNE-2Z cells ($n = 12$, $P < 0.01$). The inhibition of background chloride currents in NP69-SV40T and CNE-2Z cells was 40.5% and 70.6%, respectively (Fig. 6A and B).

ClC-3 siRNA treatments not only decreased background chloride currents, but also inhibited the chloride currents induced by 47% hypotonic solution. The whole cell recordings showed that the hypotonicity-activated chloride current in CNE-2Z cells was inhibited by ClC-3 siRNA by 57% (from 80.5 ± 6.7 pA/pF to 34.6 ± 5.1 pA/pF at +80 mV, $n = 9$, 12, $P < 0.01$), while that in NP69-SV40T cells only by 18.7% (from 40.1 ± 4.3 pA/pF to 32.6 ± 4.3 pA/pF; $n = 11$, 10, $P < 0.01$) (Fig. 6A and C). The above results indicated that the effect of ClC-3 siRNA was more pronounced in cancerous cells than in normal cells.

3.6. Effects of knock-down of ClC-3 protein expression on regulatory volume decrease (RVD) of normal and cancerous nasopharyngeal epithelial cells

Cells were treated with 100 nM ClC-3 siRNA or control siRNA in the presence of the transfection reagent lipofectamine 2000 for 48 h. The results showed that incubation of cells with specific ClC-3 siRNA significantly inhibited the RVD induced by 47% hypotonic challenges in NP69-SV40T and CNE-2Z cells (Fig. 7). However, the inhibitory effect of ClC-3 siRNA treatments on the hypotonicity-induced RVD in CNE-2Z cells was significantly stronger than that in NP69-SV40T cells. Compared to the control, the capacity of RVD was decreased by 26.6% in NP69-SV40T cells (from 23.3 ± 5.4% to 17.1 ± 5.2%, 21 cells in 3 experiments) and by 70.5% in CNE-2Z cells (from 51.6 ± 4.8% to 15.2 ± 4.4%, 20 cells in 3 experiments). The treatments with the nonsense control siRNA did not significantly change the RVD process in both cells. In the experiments, only the cells with fluorescence, indicating successful transfection of siRNA, were selected for RVD measurements.

3.7. Effect of knock-down of ClC-3 protein expression on proliferation of normal and cancerous nasopharyngeal epithelial cells

The effects of knock-down of ClC-3 protein expression by ClC-3 siRNA on cell proliferation were detected by MTT assay. Cells were treated with ClC-3 siRNA or control siRNA in the presence of the transfection reagent lipofectamine 2000 for 48 h. The results clearly indicated that proliferation of CNE-2Z cells was inhibited by ClC-3 siRNA in a dose-dependent manner (Fig. 8). Proliferation of NP69-SV40T cells was also suppressed by ClC-3 siRNA treatments. However, sensitivity of the two cell lines to ClC-3 siRNA was different. The inhibitory effect was much weaker in NP69-SV40T cells than in CNE-2Z cells. 48 h treatments with ClC-3 siRNA (100 nM) inhibited proliferation of CNE-2Z cells by 46.1 ± 5.8% ($n = 3$), while cell proliferation was suppressed only by 25.3 ± 4.6% ($n = 3$) in NP69-SV40T cells. The results suggest that the proliferation of cancer cells is more dependent on ClC-3 protein expression than that of normal cells. The treatments with 100 nM control siRNA in the presence of the transfection reagent lipofectamine 2000 for 48 h did not significantly affect proliferation of both cells.

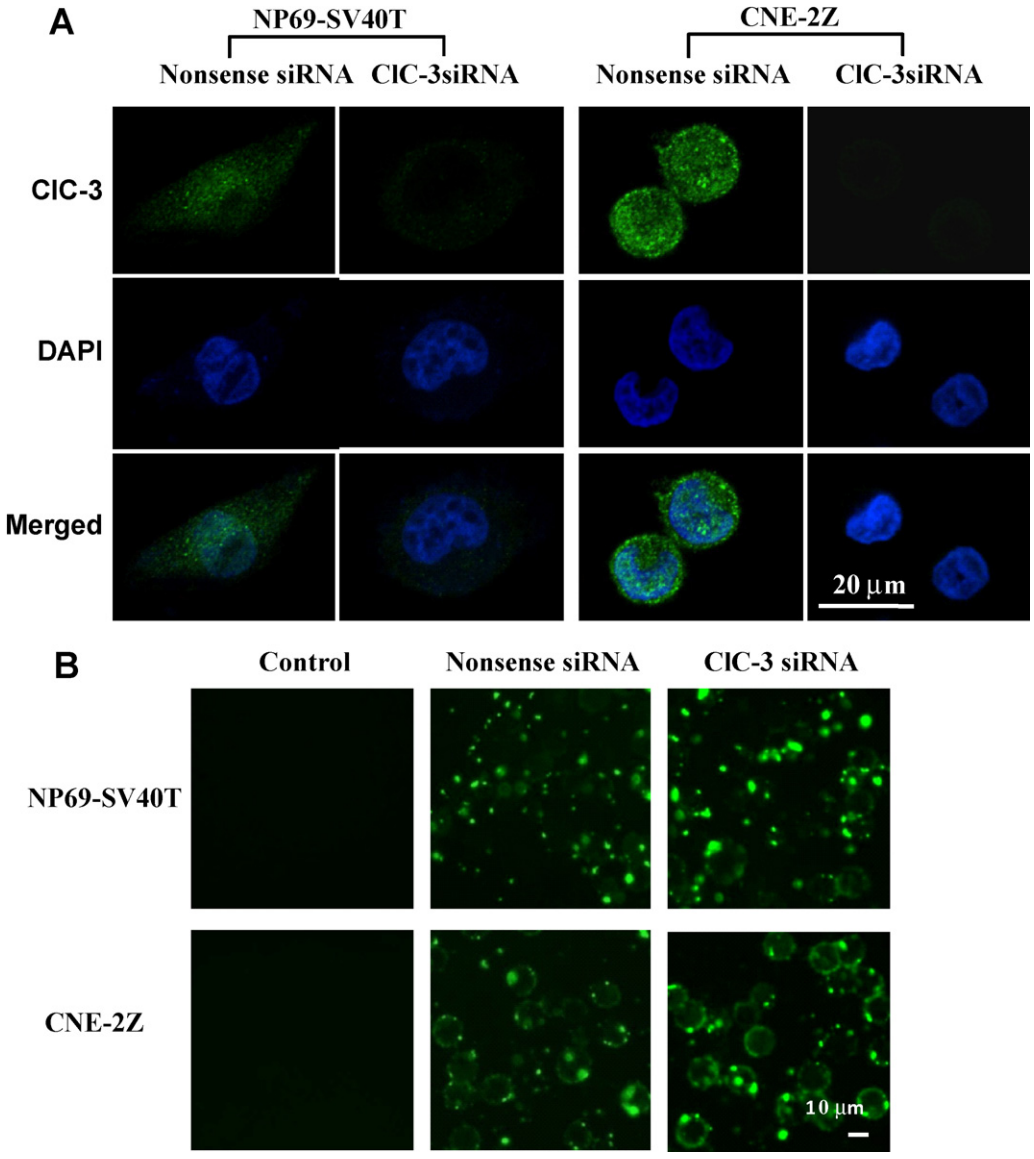

Fig. 5. Endogenous expression and knock-down of expression of ClC-3 by ClC-3 siRNA in CNE-2Z and NP69-SV40T cells. Cells were treated with 100 nM ClC-3 siRNA or nonsense siRNA in the presence of the transfection reagent lipofectamine 2000 (1 μl in 500 μl medium for 24-well plate) for 48 h. (A) ClC-3 immunofluorescence in control cells (nonsense siRNA) and the cells treated with ClC-3 siRNA (ClC-3 siRNA), and the nuclei labeled by DAPI staining. (B) The uptake of nonsense and ClC-3 siRNAs which were labeled with FAM fluorescence.

4. Discussion

In this study, the NP69-SV40T cell, a cell line derived from the normal human nasopharyngeal epithelium, and the CNE-2Z cell, a cell line developed from the human poorly differentiated nasopharyngeal epithelial carcinoma, were used. These two cell lines represent different carcinogenic potential. We found that the functional activities and expression of volume-sensitive chloride channels were different between the normal epithelial cells and the cancerous cells; proliferation of cancerous cells was more dependent on the activities of volume-sensitive chloride channels.

We found first that the CNE-2Z cell, with higher growth ability, was more sensitive to the chloride channel blockers NPPB and tamoxifen than the NP69-SV40T cell, which proliferated slower. The blockers inhibited the growth of both cells, but the degree of inhibition in the cancerous CNE-2Z cell was much higher than that in the normal NP69-SV40T cell. The result suggests that the functional activities or the expression of chloride channels were up-regulated in cancerous cells and chloride channels play a much more important role in controlling cancerous cell proliferation. The up-regulation of chloride channel activities and expression was confirmed by our further experiments. It was found that the hypotonicity-activated chloride currents, representing the functional activities of the volume-activated chloride channels, and the capability of regulatory volume decrease, which is associated with the activation of the chloride channels, were all more pronounced in CNE-2Z cells than in NP69-SV40T cells. It was also proved by us that the basic activities of chloride channels were elevated in the cancerous cells under the normal isotonic condition. We found that the background chloride current was larger in CNE-2Z cells. Suppression of the background current by the chloride channel blockers NPPB and tamoxifen led to an increase of cell volume in both cells, but the impact of the blockers on CNE-2Z cells was greater. Moreover, the endogenous expression of ClC-3 protein, a candidate of volume-activated chloride channels, was up-regulated in CNE-2Z cells. All these data indicate that chloride channel activities and expression are up-regulated in cancerous cells.

What is the significance of up-regulation of chloride channel activities? We found that functional blockages of chloride channels

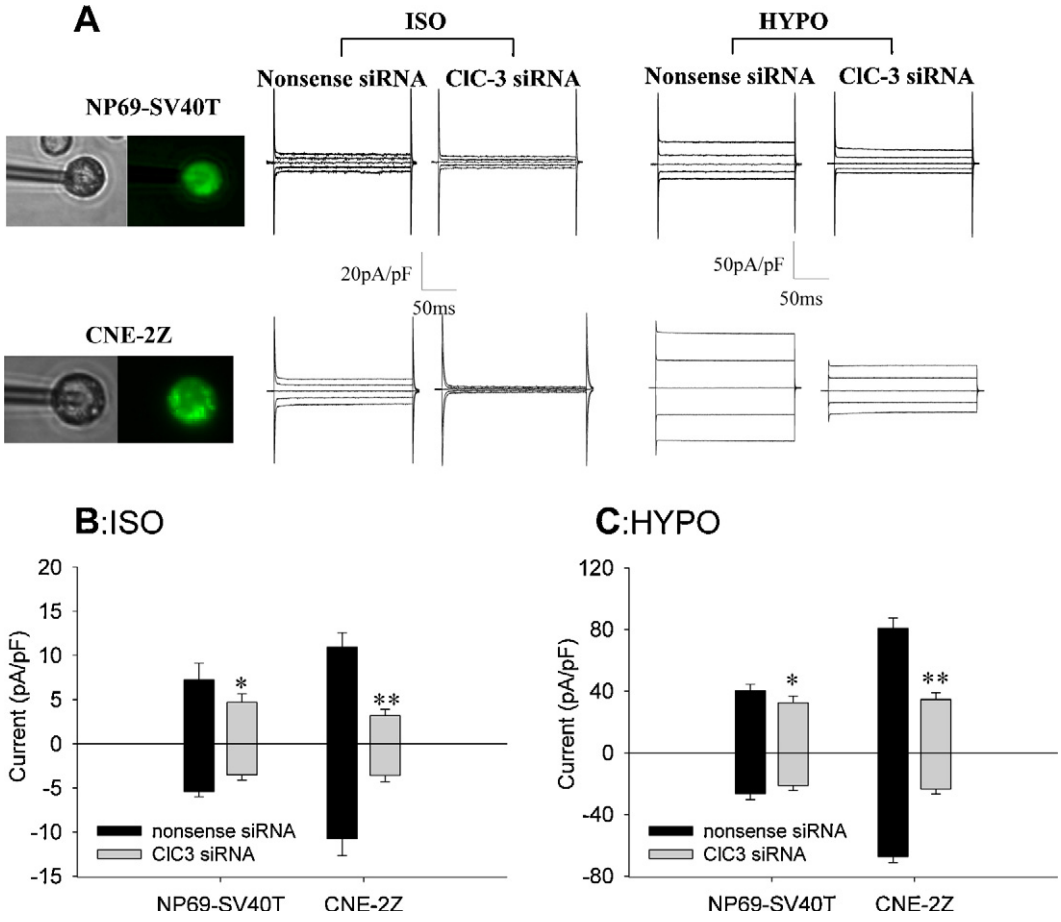

Fig. 6. Suppression of background and hypotonicity-induced chloride currents by silence of ClC-3 expression in NP69-SV40T and CNE-2Z cells. Cells were treated with 100 nM ClC-3 siRNA or nonsense siRNA in the presence of the transfection reagent lipofectamine 2000 (1 μl in 500 μl medium for 24-well plate) for 48 h. The cells with fluorescence, indicating successful transfection with siRNA, were selected for current recordings (shown in the inserts). A presents the typical current traces of background currents under isotonic conditions (ISO) and the chloride currents induced by 47% hypotonic bath solution (HYPO) in the cells treated with nonsense or ClC-3 siRNA for 48 h. (B and C) The densities of background (B) and hypotonicity-induced (C) chloride currents recorded at ±80 mV (mean ± standard error, n = 10–12). $^{*}P < 0.05$, $^{**}P < 0.01$ (*vs* nonsense siRNA).

by the chloride channel inhibitors NPPB and tamoxifen or silencing of chloride channel expression by ClC-3 siRNA significantly inhibited the proliferation of CNE-2Z cells, but only slightly affected the growth of NP69-SV40T cells. Ion channels have been suggested to be related with cancer development [31]. Our previous work demonstrated that the activities of volume-activated chloride channels and the expression of ClC-3 chloride channels were cell cycle-dependent [14,22]; cell proliferation was positively correlated with the level of volume-activated Cl^- currents and RVD [15]; suppression of ClC-3 channel expression reduces nasopharyngeal carcinoma cell migration [32]. It has also been reported by others that proliferating cells express high levels of ClC-3 proteins [19,33,34]. These data suggest that chloride channels play important roles in growth of cancerous cells and

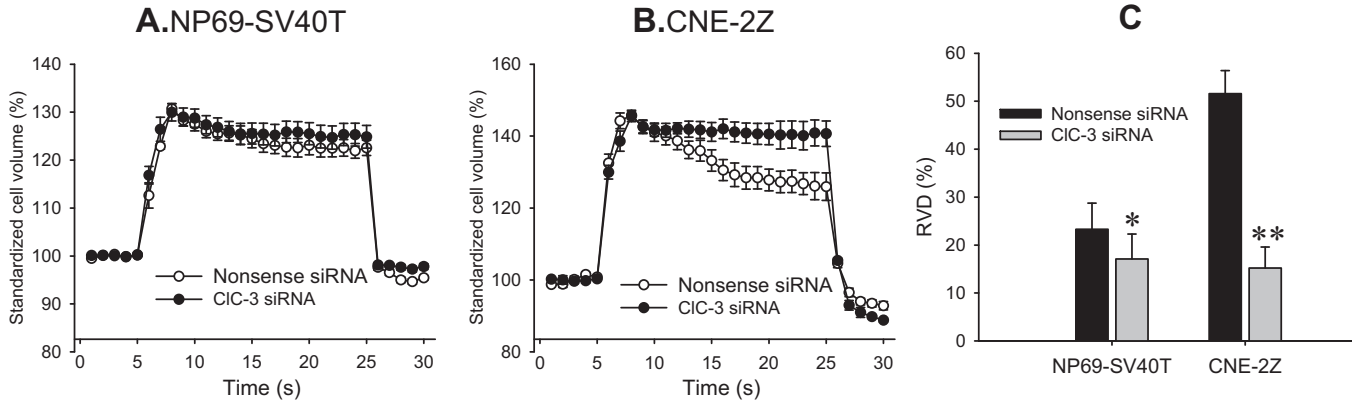

Fig. 7. Inhibition of RVD by silencing of ClC-3 expression in NP69-SV40T and CNE-2Z cells. (A and B) The changes of cell volume in the isotonic and hypotonic bath solutions when treated with negative control siRNA (nonsense siRNA, 100 nM) or with ClC-3 siRNA (ClC-3 siRNA, 100 nM) for 48 h in NP69-SV40T (n = 18 and 21) and CNE-2Z cells (n = 16 and 20), respectively. (C) The RVD capacity of both cells after treated with nonsense siRNA or ClC-3 siRNAfor 48 h. Note the higher sensitivity of CNE-2Z cells to the ClC-3 treatment, compared with NP69-SV40T cells. The data in the figures are mean ± standard error of 16–21 cells. $^{*}P < 0.05$, $^{**}P < 0.01$ (*vs* nonsense siRNA).

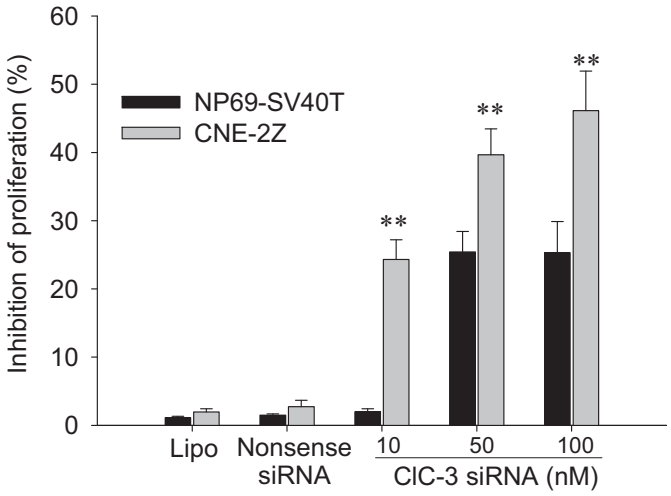

Fig. 8. Inhibition of cell proliferation by ClC-3 siRNA in NP69-SV40T and CNE-2Z cells. Cells were incubated in the medium containing the transfection reagent lipofectamine 2000 (Lipo, 0.25 μl in 100 μl medium for 96-well plate) or treated with 10, 50 and 100 nM ClC-3 siRNA or 100 nM nonsense siRNA in the presence of lipofectamine 2000 for 48 h. ClC-3 siRNA inhibited dose-dependent cell proliferation in both cells, but CNE-2Z cells were more sensitive to the treatments (mean ± standard error, $n = 3$). $^{**}P < 0.01$ (*vs* NP69-SV40T).

may contribute to the development of cancers. Chloride channels may become new targets of chemotherapy.

Why should cancerous cells up-regulate the expression of volume-sensitive chloride channels? The maintenance of cell volume is a fundamental property of mammalian cells. Metabolism, mitosis, cell growth and migration necessarily perturb the cell volume homeostasis and thus mechanisms need to be in place to compensate for these imbalances [2,3]. Many studies including our own demonstrated that activation of volume-activated chloride channels is a key mechanism for RVD [21,30,35]. In the present study, we found that RVD capability was enhanced in cancerous cells together with the up-regulation of expression of volume-activated chloride channels. These additional chloride channels improve RVD, which helps cells to survive the harsh changes occurring during rapid proliferation. RVD may ensure that concentrations of critical factors are maintained, including cyclin/cyclin dependent kinase (CDK) and other important factors needed for regulating cell cycle progression [36,37]. The involvement of chloride channels in maintenance of cell volume under normotonic conditions was confirmed by us previously [36] and in this study by the evidence that inhibition of background chloride currents by the chloride channel blockers NPPB and tamoxifen significantly increased cell volume, especially in cancerous cells.

Chloride channels may also regulate cell proliferation by affecting the expression of cell cycle regulators or by regulating the intracellular pH and ion concentrations. It was reported that silencing of ClC-3 expression down-regulates expression of the cell cycle regulators, cyclin D1 and cyclin E, and inhibits cell proliferation and cell cycle progress [38]. It has been demonstrated by us and others that ClC-3 proteins distribute mainly in nuclei and intracellular vesicles, as well as on the cell membrane [26]; ClC-3 is involved in regulation of intracellular compartment or endosomal acidification and chloride accumulation [39,40]. Another possible mechanism for the action of chloride channels is their involvement in regulation of cytoplasmatic condensation prior to cell division. It has been shown that cytoplasmic condensation (also called premitotic condensation, PMC) is an obligatory step in cell replication and is linked to chromatin condensation; PMC is dependent on ClC-3 channel function [23].

In this study, the inhibition percentages of the background and hypotonicity-activated currents caused by the chloride channel blockers NPPB and tamoxifen were slightly higher in CNE-2Z cells than in NP69-SV40T cells. This result implies that there is a greater portion of current independent of NPPB or tamoxifen-sensitive channels contributing to the signal in normal cells when compared to cancerous cells. The blocker-insensitive portion of the currents may be non-chloride background currents or may be produced by the activities of NPPB and tamoxifen-insensitive chloride channels. Comparisons of siRNA effects with those of chloride channel blockers in CNE-2Z and NP69-SV40T cells indicated that the difference of current inhibition (including inhibition of background and hypotonicity-activated currents) between the two cells were more important in siRNA experiments than in channel blocker experiments. In siRNA experiments, the effects of siRNA on cancerous were much stronger than those on normal cells. In the blocker experiments, the effects of chloride channel blockers NPPB and tamoxifen on the cancerous cells were only slightly higher than those on normal cells. These results suggest that there are more non-ClC3 chloride currents in normal cells although we cannot exclude the existence of non-ClC3 chloride currents in cancerous cells. We also showed previously that ClC-3 antisense oligonucleotides inhibited CNE-2Z cell proliferation and chloride currents. The inhibition rates were similar to those in this study, but the working concentrations of antisense oligonucleotides were much higher than those of siRNA.

As a summary, the functional activities and expression of volume-activated chloride channels are different between the cancerous nasopharyngeal epithelial cell CNE-2Z and its counterpart, the normal nasopharyngeal epithelial cell NP69-SV40T. The activities and expression of the chloride channels are up-regulated in the cancerous cells. Functional blockages of chloride channels or silencing of the expression of ClC-3, a candidate of volume-activated chloride channels, inhibited the proliferation of the cancerous and normal nasopharyngeal epithelial cells, but the cancerous cells are far more sensitive to the treatments than the normal cells. Our results strongly suggest that the activation of volume-activated chloride channels is associated with malignant behaviors of human nasopharyngeal epithelial cells; ClC-3 chloride channel may be considered as a potential tumor marker and therapeutic target for human nasopharyngeal carcinoma.

Conflicts of interest

No potential conflicts of interest were disclosed.

Grant support

This work was supported by the National Natural Science Foundation of China (Nos. 30771106, 30870567, 30871267, 31070997, 90913020 and U0932004).

References

[1] Lang F, Busch GL, Ritter M, Volkl H, Waldegger S, Gulbins E, et al. Functional significance of cell volume regulatory mechanisms. Physiol Rev 1998;78:247–306.
[2] Kunzelmann K. Ion channels and cancer. J Membr Biol 2005;205:159–73.
[3] Prevarskaya N, Skryma R, Shuba Y. Ion channels and the hallmarks of cancer. Trends Mol Med 2010;16:107–21.
[4] Hemmerlein B, Weseloh RM, Mello de Queiroz F, Knotgen H, Sanchez A, Rubio ME, et al. Overexpression of Eag1 potassium channels in clinical tumours. Mol Cancer 2006;5:41.
[5] Lu L, Yang T, Markakis D, Guggino WB, Craig RW. Alterations in a voltage-gated K^+ current during the differentiation of ML-1 human myeloblastic leukemia cells. J Membr Biol 1993;132:267–74.
[6] Huang L, Li B, Li W, Guo H, Zou F. ATP-sensitive potassium channels control glioma cells proliferation by regulating ERK activity. Carcinogenesis 2009;30:737–44.

[7] Schlichter LC, Sakellaropoulos G, Ballyk B, Pennefather PS, Phipps DJ. Properties of K^+ and Cl^- channels and their involvement in proliferation of rat microglial cells. Glia 1996;17:225–36.
[8] Rouzaire-Dubois B, Milandri JB, Bostel S, Dubois JM. Control of cell proliferation by cell volume alterations in rat C6 glioma cells. Pflugers Arch 2000;440:881–8.
[9] Gerard V, Rouzaire-Dubois B, Dilda P, Dubois JM. Alterations of ionic membrane permeabilities in multidrug-resistant neuroblastoma × glioma hybrid cells. J Exp Biol 1998;201:21–31.
[10] Voets T, Szucs G, Droogmans G, Nilius B. Blockers of volume-activated Cl^- currents inhibit endothelial cell proliferation. Pflugers Arch 1995;431:132–4.
[11] Wondergem R, Gong W, Monen SH, Dooley SN, Gonce JL, Conner TD, et al. Blocking swelling-activated chloride current inhibits mouse liver cell proliferation. J Physiol 2001;532:661–72.
[12] Phipps DJ, Branch DR, Schlichter LC. Chloride-channel block inhibits T lymphocyte activation and signalling. Cell Signal 1996;8:141–9.
[13] Shen MR, Droogmans G, Eggermont J, Voets T, Ellory JC, Nilius B. Differential expression of volume-regulated anion channels during cell cycle progression of human cervical cancer cells. J Physiol 2000;529(Pt 2):385–94.
[14] Chen L, Wang L, Zhu L, Nie S, Zhang J, Zhong P, et al. Cell cycle-dependent expression of volume-activated chloride currents in nasopharyngeal carcinoma cells. Am J Physiol Cell Physiol 2002;283:C1313–23.
[15] Chen LX, Zhu LY, Jacob TJ, Wang LW. Roles of volume-activated Cl^- currents and regulatory volume decrease in the cell cycle and proliferation in nasopharyngeal carcinoma cells. Cell Prolif 2007;40:253–67.
[16] Duan D, Winter C, Cowley S, Hume JR, Horowitz B. Molecular identification of a volume-regulated chloride channel. Nature 1997;390:417–21.
[17] Wang L, Chen L, Jacob TJ. The role of ClC-3 in volume-activated chloride currents and volume regulation in bovine epithelial cells demonstrated by antisense inhibition. J Physiol 2000;524(Pt. 1):63–75.
[18] Hermoso M, Satterwhite CM, Andrade YN, Hidalgo J, Wilson SM, Horowitz B, et al. ClC-3 is a fundamental molecular component of volume-sensitive outwardly rectifying Cl^- channels and volume regulation in HeLa cells and *Xenopus laevis* oocytes. J Biol Chem 2002;277:40066–74.
[19] Lemonnier L, Shuba Y, Crepin A, Roudbaraki M, Slomianny C, Mauroy B, et al. BCl-2-dependent modulation of swelling-activated Cl^- current and ClC-3 expression in human prostate cancer epithelial cells. Cancer Res 2004;64:4841–8.
[20] Salazar G, Love R, Styers ML, Werner E, Peden A, Rodriguez S, et al. AP-3-dependent mechanisms control the targeting of a chloride channel (ClC-3) in neuronal and non-neuronal cells. J Biol Chem 2004;279:25430–9.
[21] Ernest NJ, Weaver AK, Van Duyn LB, Sontheimer HW. Relative contribution of chloride channels and transporters to regulatory volume decrease in human glioma cells. Am J Physiol Cell Physiol 2005;288:C1451–60.
[22] Wang LW, Chen LX, Jacob T. ClC-3 expression in the cell cycle of nasopharyngeal carcinoma cells. Sheng Li Xue Bao 2004;56:230–6.
[23] Habela CW, Olsen ML, Sontheimer H. ClC3 is a critical regulator of the cell cycle in normal and malignant glial cells. J Neurosci 2008;28:9205–17.
[24] Xu B, Mao J, Wang L, Zhu L, Li H, Wang W, et al. ClC-3 chloride channels are essential for cell proliferation and cell cycle progression in nasopharyngeal carcinoma cells. Acta Biochim Biophys Sin 2010;42:370–80.
[25] Dickerson LW, Bonthius DJ, Schutte BC, Yang B, Barna TJ, Bailey MC, et al. Altered GABAergic function accompanies hippocampal degeneration in mice lacking ClC-3 voltage-gated chloride channels. Brain Res 2002;958:227–50.
[26] Stobrawa SM, Breiderhoff T, Takamori S, Engel D, Schweizer M, Zdebik AA, et al. Disruption of ClC-3, a chloride channel expressed on synaptic vesicles, leads to a loss of the hippocampus. Neuron 2001;29:185–96.
[27] Yoshikawa M, Uchida S, Ezaki J, Rai T, Hayama A, Kobayashi K, et al. CLC-3 deficiency leads to phenotypes similar to human neuronal ceroid lipofuscinosis. Genes Cells 2002;7:597–605.
[28] Tsao SW, Wang X, Liu Y, Cheung YC, Feng H, Zheng Z, et al. Establishment of two immortalized nasopharyngeal epithelial cell lines using SV40 large T and HPV16E6/E7 viral oncogenes. Biochim Biophys Acta 2002;1590:150–8.
[29] Zhang H, Tsao SW, Jin C, Strombeck B, Yuen PW, Kwong YL, et al. Sequential cytogenetic and molecular cytogenetic characterization of an SV40T-immortalized nasopharyngeal cell line transformed by Epstein-Barr virus latent membrane protein-1 gene. Cancer Genet Cytogenet 2004;150:144–52.
[30] Wang L, Chen L, Zhu L, Rawle M, Nie S, Zhang J, et al. Regulatory volume decrease is actively modulated during the cell cycle. J Cell Physiol 2002;193:110–9.
[31] Arcangeli A, Crociani O, Lastraioli E, Masi A, Pillozzi S, Becchetti A. Targeting ion channels in cancer: a novel frontier in antineoplastic therapy. Curr Med Chem 2009;16:66–93.
[32] Mao J, Chen L, Xu B, Wang L, Li H, Guo J, et al. Suppression of ClC-3 channel expression reduces migration of nasopharyngeal carcinoma cells. Biochem Pharmacol 2008;75:1706–16.
[33] Wang GL, Wang XR, Lin MJ, He H, Lan XJ, Guan YY. Deficiency in ClC-3 chloride channels prevents rat aortic smooth muscle cell proliferation. Circ Res 2002;91:E28–32.
[34] Dai YP, Bongalon S, Hatton WJ, Hume JR, Yamboliev IA. ClC-3 chloride channel is upregulated by hypertrophy and inflammation in rat and canine pulmonary artery. Br J Pharmacol 2005;145:5–14.
[35] Lemonnier L, Lazarenko R, Shuba Y, Thebault S, Roudbaraki M, Lepage G, et al. Alterations in the regulatory volume decrease (RVD) and swelling-activated Cl^- current associated with neuroendocrine differentiation of prostate cancer epithelial cells. Endocr Relat Cancer 2005;12:335–49.
[36] Nilius B. Chloride channels go cell cycling. J Physiol 2001;532:581.
[37] Lamb FS, Clayton GH, Liu BX, Smith RL, Barna TJ, Schutte BC. Expression of CLCN voltage-gated chloride channel genes in human blood vessels. J Mol Cell Cardiol 1999;31:657–66.
[38] Tang YB, Liu YJ, Zhou JG, Wang GL, Qiu QY, Guan YY. Silence of ClC-3 chloride channel inhibits cell proliferation and the cell cycle via G/S phase arrest in rat basilar arterial smooth muscle cells. Cell Prolif 2008;41:775–85.
[39] Weylandt KH, Nebrig M, Jansen-Rosseck N, Amey JS, Carmena D, Wiedenmann B, et al. ClC-3 expression enhances etoposide resistance by increasing acidification of the late endocytic compartment. Mol Cancer Ther 2007;6:979–86.
[40] Hara-Chikuma M, Yang B, Sonawane ND, Sasaki S, Uchida S, Verkman AS. ClC-3 chloride channels facilitate endosomal acidification and chloride accumulation. J Biol Chem 2005;280:1241–7.